A comparative investigation on the optical conductivity of Mg and Sn doped ZnO nanoparticles in UV regime

A. A. Jacob [a], L. Balakrishnan [b,*]
[a] *Faculty of Engineering, Emirates Aviation University, Dubai, UAE.*
[b] *Department of Physics, Government College of Technology, Coimbatore 641 013, India*

This study investigates the optical properties of zinc oxide (ZnO) nanoparticles, doped with Mg and Sn, to enhance optical conductivity in the UV regime. ZnO was synthesized via co-precipitation, and structural analysis confirmed the retention of its hexagonal wurtzite structure. Using scanning electron microscopy and energy dispersive spectroscopy, morphological and elemental analysis of the synthesized nanoparticles were studied, respectively. Optical analysis via UV-vis-NIR spectroscopy revealed a blue shift in absorbance, indicating an increase in bandgap with higher doping concentrations. The results show that small Sn doping enhances optical conductivity more effectively than higher Mg doping.

(Received January 20, 2025; Accepted May 2, 2025)

Keywords: Semiconductors, ZnO, Optical Conductivity, Band gap

1. Introduction

Zinc oxide (ZnO), a wide bandgap semiconductor with excellent UV absorption is well demanded for optoelectronic devices like LEDs, photodetectors, etc. in the UV regime. The applications of such devices are very large in environmental monitoring, flame detection and communication systems. The high exciton binding energy and nanostructured designs on the ZnO (e.g. nanorods, nanoflakes) make it uniquely suited for optical detection. Driven by recent advances of scalable fabrication methods including hydrothermal growth and solution processed thin films, these are cost effective and high-efficient solutions. ZnO and its alloys (such as ZnMgO) have revolutionized UV sensing technologies creating an alternative to traditional materials like aluminum gallium nitride. ZnO's potential in highly sensitive and stable UV photodetectors for a wide variety of applications is highlighted by these developments. A fair number of studies on the application of ZnO for UV detection had been reported and still researchers are focusing on the enhancement of optical properties for further improvements [1-3]. Doping with suitable dopants is one among the right methods to tune the optical properties of ZnO. Lower wavelength shift in the ZnO band gap is preferred for UV applications which further widen the absorption to deep UV regime [4-5]. Mg and Sn has been chosen as dopants because the incorporation of these dopants into ZnO lattice leads to the formation of intermediate complex line MgO and SnO which has higher band gap (MgO - 7.8 eV, SnO - 3.8 eV) compared to ZnO (3.37 eV). Also, the ionic radii of Mg^{2+} (0.72 Å) and Sn^{4+} (0.69 Å) in hexagonal coordination are comparable with that of Zn^{2+} (0.74 Å) such that they can replace Zn^{2+} without introducing much lattice distortion [6-7]. It is also proved that doping of Mg in ZnO nanostructure improves UV photoluminescence emission and reduces deep level emissions [5, 8]. Sn^{4+} in ZnO lattice possesses two excess electrons which leads high electrical and optical conductivity. Being a doubly ionized donor and possessing less ionization energy it improves both bandgap and optical conductivity in the host material. Further, it enhances field emission, conductivity, and luminescence properties of ZnO and produces constant optical conductivity because the induced charges are being trapped by

* Corresponding author: bslv85@gmail.com
https://doi.org/10.15251/DJNB.2025.202.457

the surface states [9-10]. Thus, the studies show that both the dopants benefit in improving the opto-electronic characteristics of ZnO, eminently in the UV regime.

In this work, a detailed comparative investigation on the optical properties of Mg and Sn doped ZnO nanostructures have been performed towards the feasibility of using ZnO in UV photodetectors.

2. Experimental details

Pristine and doped ZnO nanoparticles were synthesized using co-precipitation method which is similar to the procedure reported elsewhere [11]. Magnesium chloride and tin chloride were used as the source materials in addition to zinc chloride for the synthesis of Mg and Sn doped ZnO with the ratios of $Zn_{1-x}Mg_xO$ (x = 0.05, 0.1 and 0.15) and $Zn_{1-y}Sn_yO$ (y = 0.02, 0.04 and 0.06).

The structural properties, morphology, composition and optical properties were analysed using X-ray diffraction (Model: D8 Advance, BRUKER, Germany), Raman spectroscopy, scanning electron microscopy (Zeiss EVO 18, Germany), energy dispersive spectroscopy (Zeiss EVO 18, Germany), and UV- Vis spectroscopy (JASCO-V670, Germany) in DRS (diffuse reflectance spectroscopy) mode respectively.

3. Results and discussions

The XRD patterns of $Zn_{1-x}Mg_xO$ (x = 0.05, 0.1 and 0.15) and $Zn_{1-y}Sn_yO$ (y = 0.02, 0.04 and 0.06) given in Fig. 1a shows that all the synthesised nano powders were crystallized in hexagonal wurtzite structure and are well matched with the standard available data for ZnO (JCPDS No. 36- 1451). Non-existence of secondary phases corresponding to Mg or Sn oxides point out that Mg and Sn ions have been well incorporated into the ZnO lattice without reforming its crystal structure. The sharp high intense peaks show that the samples are highly crystalline nature and also imply that the crystallinity of ZnO is maintained after Mg and Sn doping. From the XRD data, crystallite size (D) of the synthesised nanoparticles were determined from the Williamson and Hall (W-H) plot using the Cauchy-Lorentzian relation [12],

$$\beta\cos\theta = \frac{C\lambda}{D} + 4\varepsilon\sin\theta \tag{1}$$

where, ε is the micro strain, c is the shape factor (0.89), θ is the diffraction angle and β is the full width half maximum. The crystallite size of the pristine, Mg and Sn doped ZnO nanostructures were calculated in the range of 25-30 nm.

Fig. 1b shows the Raman spectra of synthesized pristine, Mg doped and Sn doped ZnO nanopowders, in the range of 300-650 cm^{-1}. The well-known first order Raman modes such as E_2(high), E_1(LO) and second order mode $2E_2$ were observed in all the samples [13]. The E_2(high) mode ascribes to the hexagonal wurtzite structure of ZnO indicates the crystalline structure of nanopowders which is in well agreement with XRD results. The E_1(LO) peak is defect induced mode arising from oxygen vacancies and Zn interstitials in the crystal [14]. $2E_2$ second order mode attributes to the zone-bounded phonon of ZnO crystals [15]. Besides these first and second order modes, furthermore modes could be seen at ~560 nm and ~645 nm which may correspond to B1(high) and TA + B1(high) silent modes of ZnO, respectively based on the reported *ab initio calculations* [13]. Raman analysis along with XRD results confirms that ZnO structure has not been noticeably altered with Mg and Sn doping.

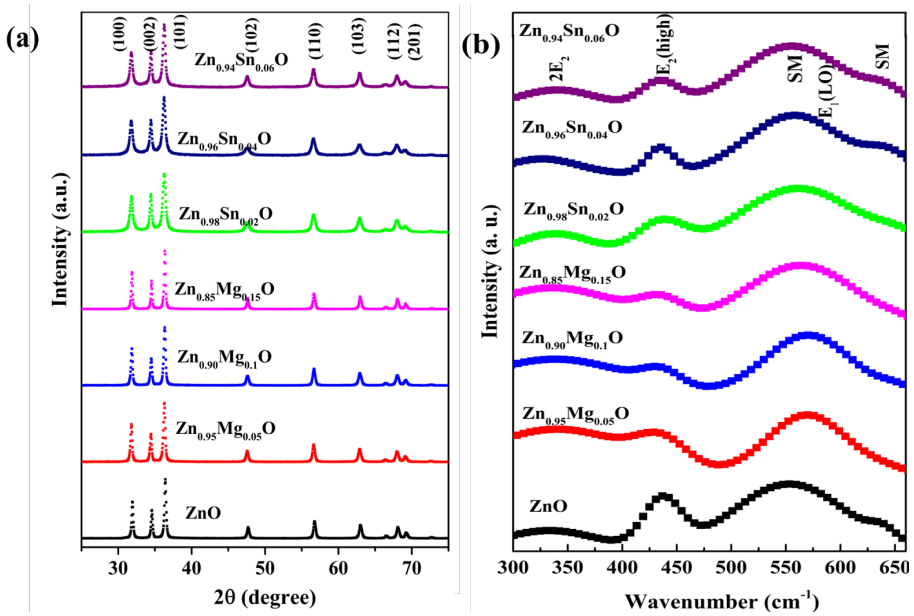

Fig. 1. (a) XRD pattern and (b) Raman Spectra of ZnO, $Zn_{1-x}Mg_xO$ and $Zn_{1-y}Sn_yO$ nanoparticles.

Fig. 2a shows the surface morphology and elemental composition data of synthesised nanoparticles analysed using SEM imaging and EDS, respectively. Nanoparticles with irregularly spherical shape and homogenous size distribution were observed. This homogeneity in particle size suggests controlled synthesis conditions and a uniform nucleation process, critical for ensuring reproducibility and desired material properties in advanced applications. From the EDS analysis, the presence of elements Mg and Sn in addition to the Zn and O has been observed in $Zn_{1-x}Mg_xO$ and $Zn_{1-y}Sn_yO$, respectively. The EDS results are in excellent agreement with the findings from the XRD analysis, which further supports the successful incorporation of Mg and Sn into the ZnO lattice without the formation of secondary phases. The absence of detectable impurities in the nanopowders ensures that the observed physical and chemical properties can be attributed solely to the intended compositional modifications, making these materials suitable for potential applications in optoelectronic and sensing devices.

The optical absorbance and reflectance spectra of the synthesised Mg and Sn doped ZnO nanopowders recorded using UV-Vis-NIR DRS is depicted in Fig. 3a and 3b, respectively and the corresponding insets shows the magnified absorbance and Kubelka monk plot. The Kubleka monk plot aids to determine the optical bandgap of materials using the relation [16],

$$F(R) = \frac{1-R^2}{2R} \tag{2}$$

where F(R) is the Kubelka Munk function and R is the reflectance. As expected, an increase in optical bandgap of ZnO was found with increasing Sn and Mg doping concentrations, also a corresponding lower wavelength shift has been observed in the absorbance which are pursuant to the previous reports [9, 17-19]. The band gap of pristine ZnO was estimated as ~3.19 eV whereas it increased to ~3.22 eV (x=0.05), 3.232 eV (x=0.10), 3.244 eV (x=0.15) for $Zn_{1-x}Mg_xO$ and to 3.210 eV (y=0.02), 3.224 eV (y=0.04) 3.226 eV (y=0.06) for $Zn_{1-y}Sn_yO$. This shows that all the synthesised nanoparticles are well suited for the light detection in UV regime among which 15% Mg exhibited relatively wide extension to UV region. The intensity of UV absorption was found to be highest for $Zn_{0.98}Sn_{0.02}O$. These results demonstrate the effectiveness of controlled doping for the purpose of changing the optical behaviour of ZnO in specific applications in UV photodetectors, optoelectronics, or any other UV related systems.

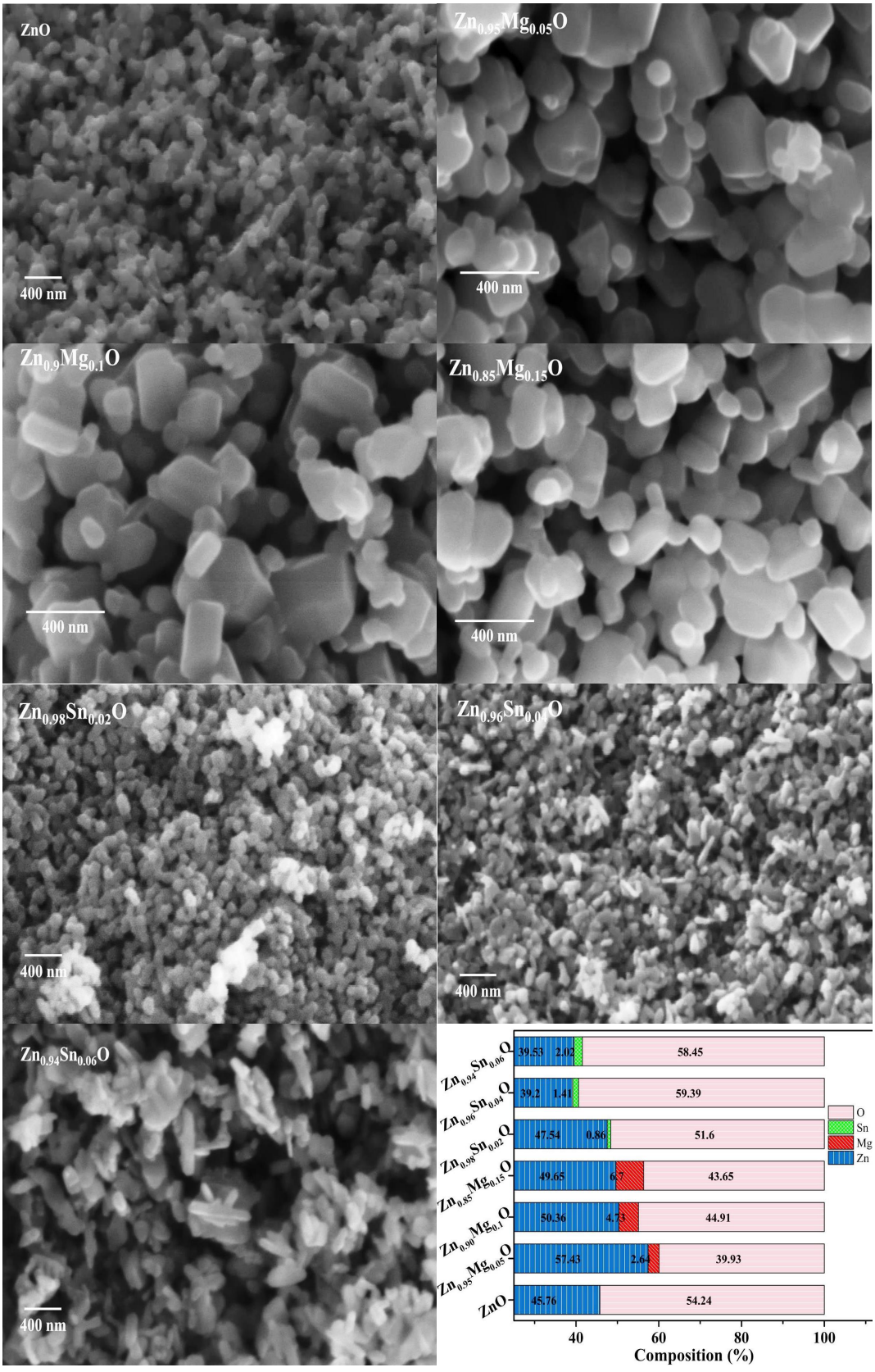

Fig. 2. SEM images and EDS data of ZnO, $Zn_{1-x}Mg_xO$ and $Zn_{1-y}Sn_yO$ nanoparticles.

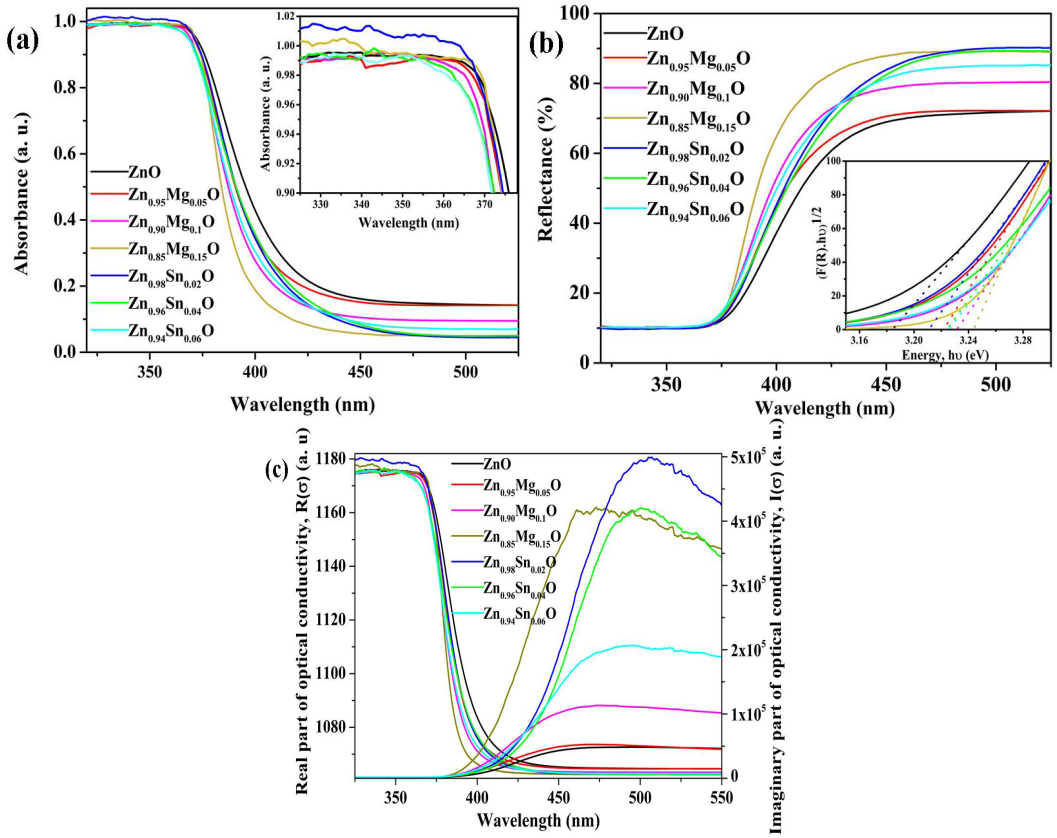

Fig. 3. (a) Optical absorption (Inset: Magnified absorption) (b) optical reflectance (Inset: Kubleka monk plot) and (c) real and imaginary part of optical conductivity of ZnO, $Zn_{1-x}Mg_xO$ and $Zn_{1-y}Sn_yO$ nanoparticles.

Further, from the DRS data, real (R(σ)) and imaginary (I(σ)) part of the optical conductivity (σ) is derived using the relations [20],

$$R(\sigma) = \omega I(\varepsilon)\varepsilon_0 \tag{3}$$

$$I(\sigma) = \omega R(\varepsilon)\varepsilon_0 \tag{4}$$

where ω = 2c/λ is the angular frequency, c is the velocity of light, R(ε), real and I(ε), imaginary part of permittivity and ε_0 is the permittivity of free space. The detailed calculation of optical parameters is reported elsewhere [21]. The variation of R(σ) and I(σ) with wavelength is shown in Fig. 3c. An increase in optical conductivity of ZnO could be seen with Mg and Sn doping. But this increase is found to be very less with Mg doping, compared to Sn doping. An appreciably large enhancement is observed with 2% Sn doping and decreases with further increase in Sn concentration. This enhancement in optical conductivity with lower concentration of Sn doping can be attributed to the doubly ionising characteristic of Sn^{4+}. With UV absorbance, the acceptor energy levels introduce in Sn doped ZnO nanostructures boost up the carrier transport and optical conductivity [10, 22]. Thus, to increase the optical conductivity of ZnO without altering its basic structure and characteristics, incorporation of Sn in small concentrations can be well preferred.

4. Conclusion

Pristine, Mg and Sn doped ZnO nanoparticles with hexagonal wurtzite structure have been synthesised by co-precipitation method. The structural integrity and crystallinity of the synthesized materials were confirmed, while the doping of Mg and Sn introduced significant modifications to their optical properties. The optical band gap of Mg and Sn doped ZnO nanostructures was found to increasing with the increase in doping concentration. All the nanoparticles exhibited excellent UV absorbance and maximum lower wavelength shift was obtained with 15% Mg doping. This significant shift highlights the potential of Mg doping to extend the UV absorption range, making $Zn_{0.85}Mg_{0.15}O$ particularly suitable for applications requiring broad UV sensitivity. Optical conductivity studies revealed that maximum improvement in UV regime optical conductivity of ZnO was obtained with 2% Sn doping. This enhancement in optical conductivity underscores the superior light-harvesting capabilities of Sn-doped ZnO nanostructures. In conclusion, while both Mg and Sn doping effectively improve the UV optical properties of ZnO, the results indicate that Sn-doped ZnO, particularly at 2% doping concentration, emerges as a more desirable candidate for the fabrication of UV photodetector with increased optical conductivity. The enhanced optical conductivity achieved with Sn doping ensures improved performance in light detection and energy conversion for advanced optoelectronic devices. Future studies could explore the integration of Mg and Sn-doped ZnO nanostructures into photodetector prototypes to evaluate their practical performance and stability under real-world conditions.

Acknowledgements

The authors are thankful to Vishnupriya, M. Sc. Project student, Vellore Institute of Technology, Vellore, Tamil Nadu, Inida-632014, who rendered her support in experimental part.

References

[1] S. Han, D.W. Yue, P. Cao, W. Liu, Y. Zeng, M. Fang, D. Zhu, Optical Materials 147, 114612. (2024); https://doi.org/10.1016/j.optmat.2023.114612

[2] E. Nurfani, L. Nulhakim, D. M. Muhammad, M. Rozana, W. Astuti, Optical Materials 148, 114948 (2024); https://doi.org/10.1016/j.optmat.2024.114948

[3] Y. Fu, L. Guo, Z. Ren Z, X. Li, Q. Zhang, J. Wu, Y. Li, W. Liu, P. Li, J. Ma, J. Hu, Ceramics International. 49 (7), 11402 (2023); https://doi.org/10.1016/j.ceramint.2022.11.339

[4] L. Sang, M. Liao, M. Sumiya, Sensors. 13, 10482 (2013); https://doi.org/10.3390/s130810482

[5] R. Viswanatha, T. G. Venkatesh, C. C. Vidyasagar, Y. A. Nayaka, Arch. Appl. Sci. Res. 4, 480 (2012); https://doi.org/10.1016/j.rinma.2020.100104

[6] O. B. Belskaya, N. N. Leont'eva, T. I. Gulyaeva, S.V.Cherepanova, V. P. Talzi, V. A. Drozdov, V. A. Likholobov, Russ. Chem. Bull. 62, 2349 (2013); https://doi.org/10.1007/s11172-013-0341-5

[7] Q. Humayun, M. Kashif, U. Hashim, J. Nanomater. 160, 792930 (2013); https://doi.org/10.1155/2013/792930

[8] A. N. Mallika, A. R. Reddy, K. S. Babu, C. Sujatha, K. V. Reddy, Opt. Mater. 36, 879 (2014); https://doi.org/10.1016/j.optmat.2013.12.015

[9] Y. Liu, X. Chen, Y. Xu, Q. Zhang, X. Wang, J. Nanomater. 2014(1), 381819 (2014); https://doi.org/10.1155/2014/381819

[10] S. K. Mishra, S. Bayan, R. Shankar, P. Chakraborty, R. K. Srivastava, Sens. Actuators. A: Phys. 211, 8 (2014); https://doi.org/10.1016/j.sna.2014.02.020

[11] A. A. Jacob, L. Balakrishnan, K, Shambavi, Z. C. Alex, RSC Adv. 7, 39657 (2017); https://doi.org/10.1039/C7RA05429G

[12] F. Yakuphanoglu, J. Alloys. Compd. 507, 184 (2010); https://doi.org/10.1016/j.jallcom.2010.07.151

[13] F. Decremps, J. Pellicer-Porres, A. M. Saitta, J. C. Chervin, A. Polian, Phys. Rev. B: Condens. Matter Mater. Phys. 65, 092101 (2002); https://doi.org/10.1103/PhysRevB.65.092101

[14] D.H. Fan, W.Z. Shen, M.J. Zheng, Y.F. Zhu, J.J. Lu, J. Phys. Chem. C 111, 9116 (2007); https://doi.org/10.1021/jp070613z

[15] G.J. Exarhos, S.K. Sharma, Thin Solid Films 270, 27 (1995); https://doi.org/10.1016/0040-6090(95)06855-4

[16] A. A. Jacob, L. Balakrishnan, S. R. Meher, K. Shambavi, Z. C, Alex, Int. J. Nanosci. 16, 1760015 (2017); https://doi.org/10.1142/S0219581X17600158

[17] M. Arshad, M. M. Ansari, A. S. Ahmed, P. Tripathi, S. S. Ashraf, A. H. Naqvi, A. Azam, J. Lumin. 161, 275 (2015); https://doi.org/10.1016/j.jlumin.2014.12.016

[18] Y. Wang, X. Zhao, L. Duan, F. Wang, H. Niu, W. Guo, A. Ali, Mater. Sci. Semicond. Process. 29, 372 (2015); https://doi.org/10.1016/j.mssp.2014.07.034

[19] S. Sakthivel, V. Baskaran, Nano Vis. 5, 157000 (2016); https://doi.org/10.1016/j.egypro.2014.07.193

[20] K. R. Raj, P. Murugakoothan, Optik 123, 1082 (2012); https://doi.org/10.1016/j.ijleo.2011.07.036

[21] A. A. Jacob, L. Balakrishnan, S. R. Meher, K. Shambavi, Z. C. Alex, J. Alloys Compd. 695, 3753 (2017); https://doi.org/10.1016/j.jallcom.2016.11.265

[22] S. Ilican, M. Caglar, Y. Caglar, Appl. Surf. Sci. 256, 7204 (2010); https://doi.org/10.1016/j.apsusc.2010.05.052